

# Material Considerations for Avalanche Photodiodes

J. P. R. David, *Senior Member, IEEE*, and C. H. Tan, *Member, IEEE*

(Invited Paper)

**Abstract**—Avalanche photodiodes (APDs) are widely used to detect and amplify weak optical signals by utilizing the impact ionization process. The choice of material is critical for the detection of a particular wavelength, and it is often expedient to use a combination of different materials to optimize the overall device performance. The APDs are now capable of covering a wide spectrum from the infrared down to the ultraviolet wavelengths. This paper will review the material requirements to achieve high gain with low excess noise at the different wavelength regions.

**Index Terms**—Avalanche multiplication, avalanche photodiodes (APDs), excess noise, impact ionization, tunneling.

## I. INTRODUCTION

AVALANCHE photodiodes (APDs) are used to detect and amplify weak optical signals using the internal gain provided by the impact ionization process. They have been used widely in optical communication systems, especially at high bit rates, as the internal gain mechanism can significantly improve the SNR of an optical receiver in which the dominant noise source is the amplifier noise [1].

Due to their smaller size, lower operating voltages, low cost, and robustness, APDs are starting to displace traditional optical amplification devices such as photomultiplier tubes (PMTs) when very high sensitivity down to single photon detection levels and high quantum efficiency (QE) are required. They are also being developed into focal plane arrays for a variety of 2-D and 3-D imaging applications where conventional detector arrays do not have the required sensitivity.

The development of new semiconductor materials and structures has opened up the possibility of APDs operating from UV to IR wavelengths. This paper will review the material requirements for high performance APDs and recent progress in new materials and structures for APDs.

## II. BACKGROUND THEORY

All APDs have similar requirements: the incident photons are detected with high QE, and the carriers created are then subjected to a sufficiently high electric field such that they undergo impact ionization and produce avalanche multiplication (or gain). To ensure a high QE, the material has to have a high absorption coefficient and be thick enough to absorb most of the incident photons. At the same time, the dark currents have to be low, something that is difficult to achieve in simple p-n

or pin diodes due to the high electric fields required. Moreover, the thickness of the structure can compromise high-speed performance.

The avalanche multiplication process provides gain, but this is usually at the expense of extra or “excess” noise that arises due to the stochastic nature of the impact ionization process. The microscopic manner in which a carrier gains energy from an electric field and undergoes impact ionization depends on the semiconductor band structure and the scattering environment it finds itself. A good review of the theory of the impact ionization process in semiconductors at low electric fields ( $<300$  kV/cm) is given by Capasso [2]. Unlike in PMTs where only electrons undergo multiplication, in semiconductors, both electrons and holes are capable of generating extra carriers when subject to a high enough electric field. The electron and hole ionization coefficients, represented by  $\alpha$  and  $\beta$ , respectively, represent the inverse of the mean distance between successive ionization events at a given applied electric field.

McIntyre showed that the noise power spectral density in an APD is given by [3]:

$$\phi = 2qI_{ph}M^2F(M)$$

where  $I_{ph}$  is the mean photocurrent and  $M$  is the mean gain.  $F(M)$  is the excess noise factor associated with  $M$  that arises from the stochastic nature of the ionization process, and McIntyre also showed that this could be expressed in the case of a uniform electric field when electrons initiate multiplication by

$$F_e(M_e) = kM_e + \left(2 - \frac{1}{M_e}\right)(1 - k).$$

And for the case when holes initiate multiplication by

$$F_h(M_h) = \frac{1}{k}M_h + \left(2 - \frac{1}{M_h}\right)\left(1 - \frac{1}{k}\right)$$

where  $k$  is the ratio of hole to electron ionization coefficients ( $\beta/\alpha$ ) in this expression, and this holds true when the ionization coefficients are in equilibrium with the electric field—the so-called “local” approximation. In most semiconductor materials, this local approximation provides an accurate prediction of the excess noise factors in for thick avalanche regions ( $>1 \mu\text{m}$ ). The effects of nonlocal behavior will be discussed in a later section. From this expression, we can see that the lowest excess noise is obtained when  $k$  is minimized for electron initiated multiplication, as shown in Fig. 1, and maximized for hole-initiated multiplication. The  $\alpha$  and  $\beta$  are determined by the band structure of the semiconductor, the scattering processes (mainly optical phonons), and the electric field. As the electric field increases, the carriers can gain energy from the field at a faster rate than they lose it to the various scattering processes, so  $\alpha$  and

Manuscript received December 18, 2007; revised January 22, 2008.

The authors are with the Department of Electronic and Electrical Engineering, University of Sheffield, Sheffield S1 3JD, U.K. (e-mail: j.p.david@sheffield.ac.uk).

Digital Object Identifier 10.1109/JSTQE.2008.918313

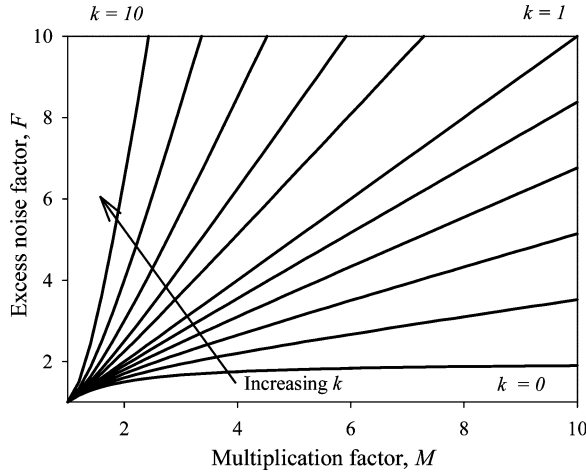


Fig. 1. Excess noise factor versus multiplication factor for different  $k$ , where  $k = 0, 0.2, 0.4, 0.6, 0.8, 1, 1.5, 2, 3, 5$ , and  $10$ .

$\beta$  increase with field and become more similar, i.e.,  $k$  tends to unity. This condition dictates the use of thick avalanche regions (hence low electric fields) in early APD designs to minimize the excess noise.

Another design consideration for APDs is that their bandwidth can be limited by the requirement of multiple transits of the avalanche region to achieve the high gain. The higher the required gain, the more transits will be required and the lower the bandwidth. However, Emmons [4] showed that this bandwidth limitation is removed when either  $\alpha$  or  $\beta = 0$ . For nonzero ionization coefficients, the frequency dependence of electron initiated mean gain is approximately given by

$$M(\omega) = \frac{M}{[1 + (\omega M k t)^2]^{0.5}} \quad M > \frac{\alpha}{\beta}$$

where  $t$  is effective carrier transit time and  $\omega$  is the signal frequency in rad/s. It is clear that for both low excess noise and for high bandwidth, a very small (or large)  $k$  is desirable using pure electron (or hole) initiated multiplication.

The requirement for high-speed APDs necessitates the use of thin avalanching regions to minimize the avalanche built up time. However the higher electric fields in thin avalanche regions lead to higher excess noise according to the McIntyre local theory. This suggests that at a given mean gain, the excess noise factor increases in thin avalanche regions. As  $\alpha$  and  $\beta$  are assumed to depend only on the local electric field, the ionization path length probability distribution function (PDF) for both electrons and holes is an exponentially decaying function of distance, and the mean ionization path length is equal to  $1/\alpha$  and  $1/\beta$ , respectively. Fig. 2 shows a schematic of this PDF for electrons.  $h_e(x)$  is the probability that a carrier will ionize at the position  $x$ , having not ionized previously in its travel. A narrow PDF with a rapid exponential decay, obtained when  $1/\alpha$  is significantly smaller than the avalanche region width  $W$ , will produce very low excess noise. Unfortunately, this condition cannot be achieved in most semiconductor materials because ionization events initiated by feedback carriers lead to avalanche breakdown when  $1/\alpha$  is comparable to  $W$ . Consequently, in

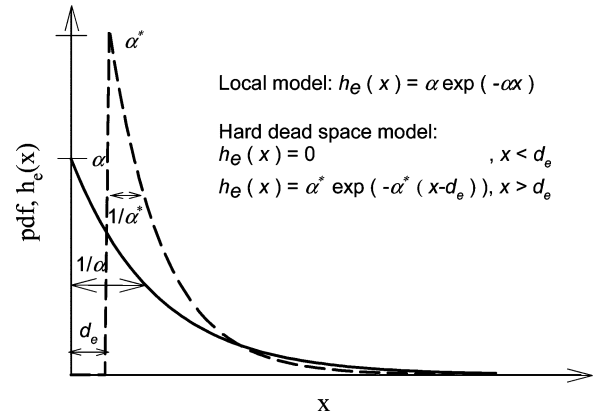


Fig. 2. PDFs of ionization path lengths in local and hard dead space models.

APDs with large  $W$ , low excess noise can only be achieved by reducing the statistical fluctuation of impact ionization via suppression of hole (or electron) ionization, when  $\beta \rightarrow 0$  (or  $\alpha \rightarrow 0$ ).

Fortunately, at higher electric fields in thin avalanching structures, the dead-space effect becomes significant, and this can reduce the excess noise substantially. The dead space  $d$  is the minimum distance that a carrier has to travel in an electric field to acquire sufficient energy to impact ionize, and this can become a significant fraction of the avalanching width. In these devices with thin avalanching widths, the ionization path length PDF can be approximated by a displaced exponential function, as shown in Fig. 2 by the dashed line. The maximum value of  $\alpha$  is now represented by  $\alpha^*$  and is sometimes referred to as the “enabled” or “microscopic” ionization coefficient. In this situation, the McIntyre local theory does not hold and analytical [5]–[7] or numerical models [8], [9] have to be used. The value of  $d$  for electrons and holes is approximately given by  $E_{th}/q\xi$ , where  $E_{th}$  is the threshold energy for ionization and depends on the semiconductor band structure,  $q$  is the electron charge, and  $\xi$  is the electric field. This dead-space effect can be quite significant and large reduction in the excess noise can occur as a result of a much narrower PDF than the local model. Therefore, APDs with low excess noise can be obtained even with  $k \sim 1$  as will be shown later.

In the following sections, we review material consideration for APDs for telecommunication, infrared, and ultraviolet applications. This will be limited to bulk or effectively bulk structures such as superlattices and avoid discussions of structures, which include band gap engineering or heterojunctions in the avalanching region [10], [11] or the more recent ionization impact engineering ( $I^2E$ ) structures [12], [13].

### III. APDs FOR TELECOMMUNICATION APPLICATION

The earliest APDs were based on silicon utilizing a reach-through structure [14] that has a relatively thin multiplication region with high electric field and a much thicker carrier drift region with lower field. This structure gives high QE, but with a relatively low operating voltage. These devices were adequate to detect light from the emitters in the first communication

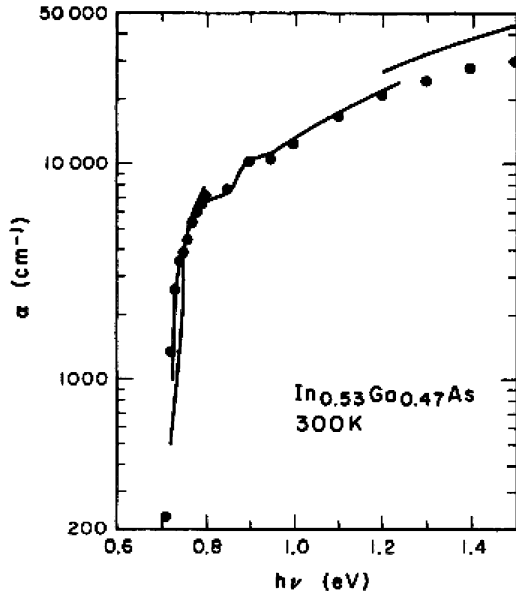


Fig. 3. 300 K absorption coefficient of  $\text{In}_{0.53}\text{Ga}_{0.47}\text{As}$  [19].

window (800–900 nm) with an enhanced sensitivity, and were fast enough for the speeds required then. Silicon has a large  $\alpha/\beta$  ratio, typically 10–100, especially at low electric fields. At the relatively modest speeds, required silicon APDs could operate with high gain and very low excess noise. As fibre-based optical communication systems evolved, there was an increasing requirement for APDs capable of detecting light at 1.3  $\mu\text{m}$  and 1.55–1.65  $\mu\text{m}$ . The earliest APDs capable of detecting photons in this wavelength range were based on Ge [15], [16], however, Ge has  $\beta/\alpha \sim 1.5$  [17], so low excess noise Ge APDs could not be obtained. Furthermore, the absorption of Ge drops off rapidly beyond 1.5  $\mu\text{m}$ , especially if it is cooled [18], and due to the narrow band gap, suffers from a high thermal generation rate.

The alloy  $\text{In}_{0.53}\text{Ga}_{0.47}\text{As}$  (or hereafter referred to as InGaAs) can be grown lattice matched on InP substrates, and is a direct band gap semiconductor with  $E_g = 0.75$  eV, enabling it to absorb photons with wavelengths up to 1.65  $\mu\text{m}$ . Fig. 3 shows the absorption coefficient of  $\text{In}_{0.53}\text{Ga}_{0.47}\text{As}$  at 300 K [19]. At a wavelength of 1.55  $\mu\text{m}$ , its absorption coefficient of 7000  $\text{cm}^{-1}$  is more than an order of magnitude larger than that of Ge [20], so that a thickness of 1.5  $\mu\text{m}$  can absorb >70% of the incident photons. This has enabled high-speed p-i-n diodes to operate at up to  $\sim 10$  GHz with a good QE. Attempts to obtain significant avalanche gain by increasing the electric field (as in Si and Ge), however, is not possible, as the onset of quantum mechanical tunneling in this material results in very high leakage currents. The tunneling current is given by [21], [22]:

$$I_{\text{tunn}} = \frac{(2m^*)^{0.5} q^3 \xi V A}{h^2 E_g^{0.5}} \exp \left[ -\frac{2\pi\sigma_T (m^*)^{0.5} E_g^{1.5}}{qh\xi} \right]$$

where  $m^*$  is the effective electron mass,  $q$  is the electron charge,  $\xi$  is the electric field,  $V$  is the applied voltage,  $A$  is the device area,  $h$  is the Planck's constant,  $E_g$  is the direct energy band gap,

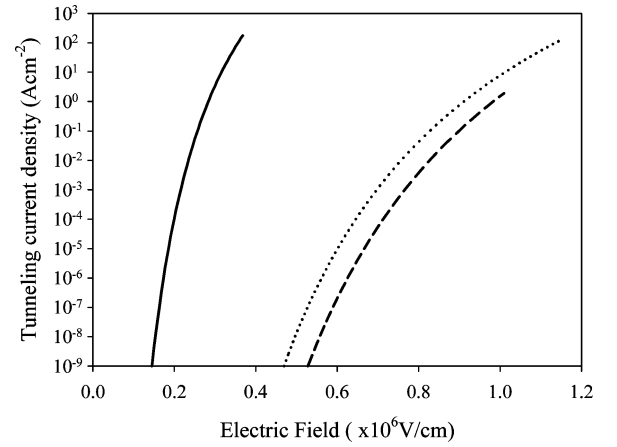


Fig. 4. Tunneling current density for InGaAs (solid line) [25], InP (dotted line) [26], and InAlAs (dashed line) [27] shown for comparison.

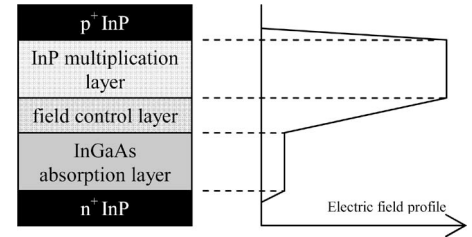


Fig. 5. Schematic of the SAM layer structure of typical InP–InGaAs APD (not to scale). Also shown is the electric field profile under normal reverse bias operation.

and  $\sigma_T$  is a constant that depends on the detailed shape of the tunneling barrier. InGaAs with its narrow band gap and small electron effective mass begins to tunnel at fields as low as 150 kV/cm [23]–[25] and increases rapidly with increasing field, as shown in Fig. 4. The tunneling current densities in InP [26] and  $\text{In}_{0.52}\text{Al}_{0.48}\text{As}$  (or InAlAs hereafter) [27] obtained from measurements on a series of submicron p-i-n diodes, are also included for comparison. Electric fields in excess of 350 kV/cm would be required for any appreciable gain in a 1- $\mu\text{m}$  thick InGaAs structure, and in such a situation, the noise performance would be dominated by the high tunneling currents.

This problem was overcome by the combination of an InGaAs region capable of absorbing photons under low electric field, and a lattice matched wider band gap InP region producing avalanche multiplication—the separate absorption and multiplication or separate absorption and multiplication avalanche photodiode (SAM-APD) [28]. Fig. 5 shows a schematic of such a structure. The high electric field exists in the wider band gap InP, where tunneling is not a serious problem (see Fig. 4), and the InGaAs experiences only a relatively low field, sufficient to sweep out photogenerated carriers. The critical part of this device is the thickness and doping in the field control layer that has to decrease the high field in the multiplication region by an appropriate amount. In all these structures, the avalanche gain and excess noise are predominantly determined by the ionization coefficients of InP [29], shown in Fig. 6. In InP,  $\beta$  is greater than  $\alpha$  over the entire electric field range studied, and

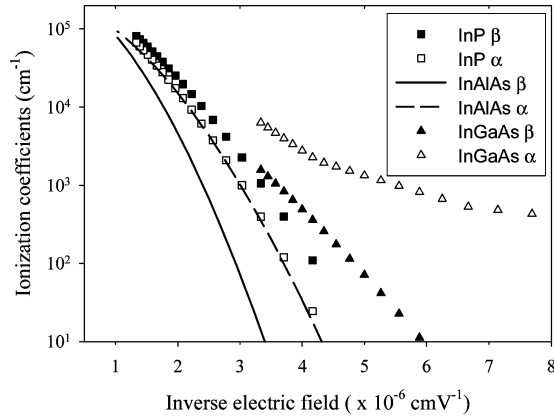


Fig. 6. Ionization coefficients of InAlAs [27], InP [29], and InGaAs [37].

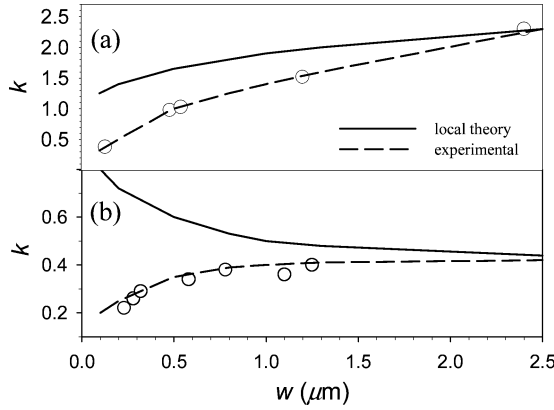


Fig. 7. Experimental effective ionization coefficient ratio in InP [26], [36] versus avalanche region thickness,  $W$ , for electron (a) and hole (b) initiated multiplication. Fittings from Tan *et al.* [26] (dashed lines) are also compared with a local model using ionisation coefficients from Cook *et al.* [29].

the  $\beta/\alpha$  ratio varies from 4 at low fields to 1.3 at the highest fields investigated. According to the McIntyre local theory, this will give rise to APDs with noise corresponding to  $1/k \sim 0.4$  in  $\sim 1\text{-}\mu\text{m}$  thick avalanching structures using hole initiated multiplication. Therefore, early designs for commercial InGaAs/InP SAM-APD employed thick InP avalanche region to keep the excess noise low.

There have been several improvements to the basic SAM-APD design over the years, such as introducing a continual or step grading in the band gap of the absorption/multiplication regions to prevent carrier trapping [30], [31], and attempts to introduce a charge or field control layer—the separated absorption charge multiplication avalanche photodiode (SACM-APD) [32]–[34]. These are described in more detail in a recent review of telecommunication APDs by Campbell [35]. The width of the InP avalanching region in these devices has continued to shrink due to the requirement for higher operating speed. Fig. 7 shows both electron and hole initiated noise performance of InP p-i-n diodes with varying avalanching widths [26], [36]. A local model (shown by the solid lines) is clearly incapable of predicting noise performance on devices with thin avalanching widths and overestimates the measured values. An InP diode with an avalanching width of  $0.25\text{ }\mu\text{m}$  would exhibit a noise

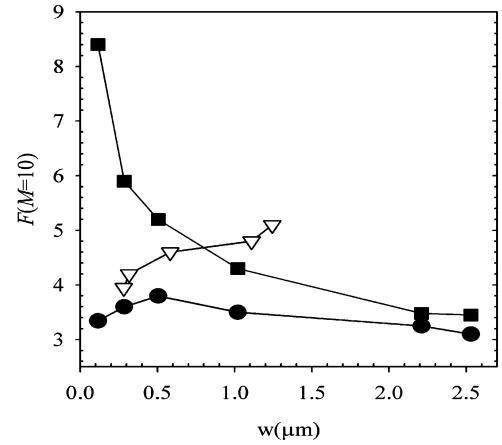


Fig. 8.  $F(M = 10)$  versus avalanche region width,  $W$ , resulting from pure electron injection (●) in  $\text{In}_{0.52}\text{Al}_{0.48}\text{As}$  diodes [43], pure hole injection in InP (▽) [36], and values predicted from the local model for  $\text{In}_{0.52}\text{Al}_{0.48}\text{As}$  (■). Lines are drawn to aid visualization.

performance equivalent of  $1/k \sim 0.25$  for hole initiated multiplication, although the actual ionization coefficient ratio at such electric fields would yield a much larger value of  $\sim 0.7$  using McIntyre's local model. This significant reduction is due to the dead space effect. Going to much thinner avalanche widths would increase the dead space effect, and hence, would continue to decrease the excess noise. However, in practice, this would incur a penalty due to an increase in the tunneling currents with electric field, as shown in Fig. 4.

The assumption that there is little or no ionization in the InGaAs absorber region of an SAM-APD structure is not necessarily true, especially if the field exceeds  $120\text{ kV/cm}$  [37], as shown in Fig. 6. Unlike other semiconductors, the  $\alpha$  in InGaAs does not decrease rapidly with decreasing field, and shows a persistent low-field ionization [38]. Since  $\alpha > \beta$  in InGaAs, electrons leaving the InP multiplication region can initiate long multiplication chains that will be detrimental to the noise and bandwidth performance of the APD [39]. Therefore, it is important to keep the electric field in the InGaAs absorber as low as possible to suppress impact ionization as well as to keep the tunneling current low.

In recent years, InAlAs, also lattice matched to InGaAs and InP, has been gaining popularity as a replacement for the InP as the multiplication region. The  $\alpha/\beta$  ratio has been found to be significantly larger than the  $\beta/\alpha$  ratio in InP [27], [40], [41] at low electric fields, as shown in Fig. 6 even though the  $\alpha$  in both materials appears to be identical. The excess noise factor at a given gain is significantly lower in InAlAs than that in InP, in both thick *and* thin avalanche regions, as shown in Fig. 8 [36], [42], [43] due to the large  $\alpha/\beta$  ratio in the former and the beneficial effect of the dead space in the latter.

Due to the slightly larger band gap in InAlAs as compared to that in InP, even higher electric fields can be applied before tunneling becomes a significant problem (see Fig. 4). Since  $\alpha > \beta$  in InAlAs, it will be holes that enter the InGaAs absorber in an SAM-APD, and as  $\beta$  is significantly lower than that of  $\alpha$ , it has little effect on the overall performance of the APD [39].

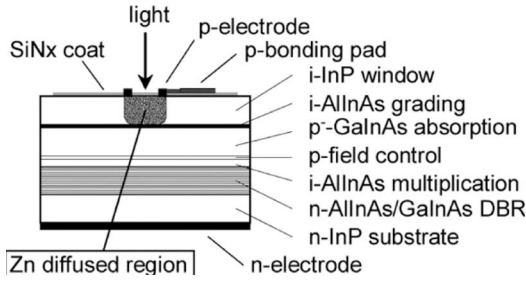


Fig. 9. Schematic cross section of the InAlAs-InGaAs APD [44].

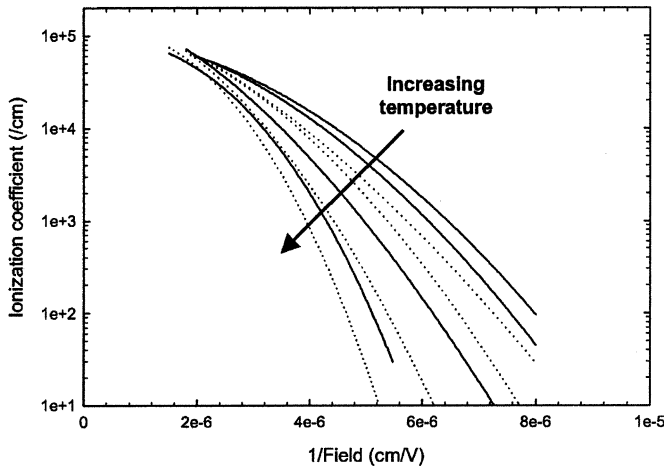


Fig. 10. Parameterized  $\alpha$  (solid lines) and  $\beta$  (dotted lines) for GaAs at 20, 77, 200, and 290 K [46].

Further advantages of the InAlAs-based APD appears to be the possibility of a planar device without the need for diffused or implanted guard rings [44], as shown in Fig. 9, and a higher gain bandwidth than InP APDs due to its larger  $\alpha/\beta$  ratio.

The impact ionization process can be sensitive to changes in temperature, primarily via changes to the phonon population. Inelastic carrier scattering at the fields typical of the ionization process is dominated by interactions with phonons, whose population,  $n$ , is given by

$$n = \left[ \exp \left( \frac{hw}{k_B T} \right) - 1 \right]^{-1}$$

where  $hw$  is the phonon energy,  $T$  is the absolute temperature in Kelvin, and  $k_B$  is Boltzmann's constant. Both the phonon energy and the details of the scattering rates are dependent on the band structure of the material, so significant differences can be found in different semiconductor materials. While the  $\alpha/\beta$  ratio in  $\text{Al}_x\text{Ga}_{1-x}\text{As}$  does not change significantly with temperature [45], the values of  $\alpha$  and  $\beta$  can change significantly [46], and consequently, affect the temperature stability of APDs. Fig. 10 shows the changes to the ionization coefficients in GaAs as the temperature decreases from room temperature to 20 K [46]. At low fields, both  $\alpha$  and  $\beta$  increase rapidly as the temperature decreases due to a reduction in the phonon scattering, which is the main energy loss mechanism at these fields. Phonon scattering is relatively less important at higher electric fields as carriers gain energy more quickly than they lose it, con-

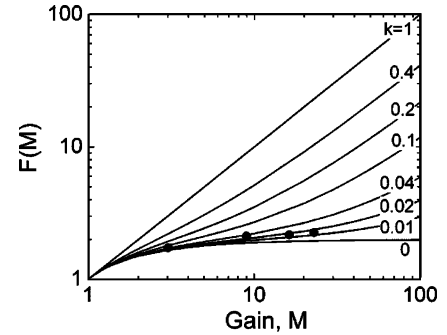


Fig. 11. Measured excess noise factors of the fused InGaAs-Si APD. The circles are the excess noise factor values obtained from measurements, and solid lines are those calculated from McIntyre's model at different  $k$  [49].

sequently changes in temperature have a much smaller effect on  $\alpha$  and  $\beta$ . The ionization behavior is consequently temperature insensitive in thin avalanching width devices where the electric fields are high. The temperature dependence of the ionization process in InAlAs is found to be much smaller than those of InP, adding to its attractiveness as a replacement for InP [47].

One interesting attempt to combine the near-IR absorption characteristics of InGaAs with the superior excess noise properties of Si involved wafer bonding of the InGaAs to Si [48], [49]. Good interfaces between the Si and InGaAs layers were obtained with no evidence of threading dislocations and devices showed low dark currents and gain of up to 130 with  $1.3 \mu\text{m}$  illumination [48]. Such devices have reported quite promising results such as a dark current of  $0.6 \text{ mA/cm}^2$  at a gain of 10, and a small excess noise of 2.3 at a gain of 20, corresponding to a  $k \sim 0.02$  [49], as shown in Fig. 11 (InGaAs on Si result). These devices also show a small change in breakdown voltage of 30–31.4 V for a  $50^\circ\text{C}$  increase in temperature, corresponding to a thermal coefficient of breakdown voltage of only  $0.09\%/^\circ\text{C}$ , but the reliability and reproducibility of the InGaAs/Si interface remains an issue for the commercial exploitation of these devices.

#### IV. INFRARED APDS

There has been relatively little work done on producing APDs that work beyond the telecommunication range of wavelengths, although there are applications in remote sensing, medical diagnostics, and environmental monitoring. Part of the problem is that the increasingly narrow band gaps required place great constraints on the choice of materials. The dark current in most narrow band gap materials is unacceptably high, and therefore, APDs using bulk materials are difficult to realize.

##### A. Sb-Based APDs

$\text{AlGaAsSb/InGaAsSb}$  heterostructures lattice matched to GaSb may be the basis of extended wavelength APDs. Sulima *et al.* [50] investigated structures of  $\text{AlGaAsSb/InGaAsSb}$  on GaSb substrates grown by liquid phase epitaxy (LPE). Although no avalanche gain was seen in that structure due to the high dark currents, a diffused p-n junction in  $\text{In}_{0.15}\text{Ga}_{0.85}\text{As}_{0.17}\text{Sb}_{0.83}$  with a band gap of 0.55 eV demonstrated avalanche gain and a

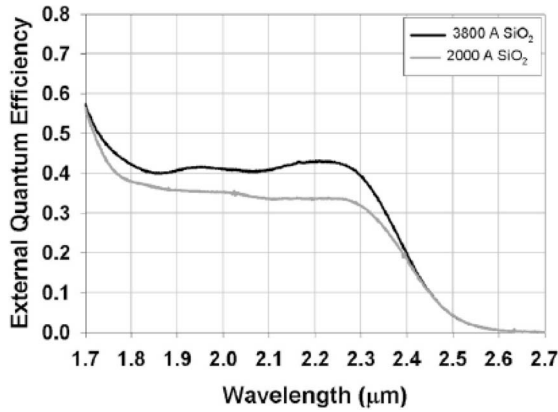


Fig. 12. Room temperature external QE versus wavelength for the Type II devices reported by Sidhu *et al.* [51], at  $-2$  V bias, with two different top surface coatings.

photoresponse from  $1.8$ – $2.2$   $\mu\text{m}$ . A multiplied responsivity of  $8.9$  A/W at  $2$   $\mu\text{m}$  was obtained; unfortunately, this was also accompanied by high dark currents. A more careful design and growth of an SAM-APD structure using wider band gap AlGaAsSb as the multiplication region may enable lower dark current devices to be produced at these wavelengths.

### B. Type II $\text{In}_{0.53}\text{Ga}_{0.47}\text{As}/\text{GaAs}_{0.51}\text{Sb}_{0.49}/\text{InP}$ SAM-APDs

Rather than use narrow band gap bulk structures, an interesting alternative technique uses Type II superlattices of  $\text{In}_{0.53}\text{Ga}_{0.47}\text{As}/\text{GaAs}_{0.51}\text{Sb}_{0.49}$  to extend the absorption region to beyond  $2$   $\mu\text{m}$  [51] with high QE, while maintaining lattice match to InP. Due to the Type II band alignment between these two materials, electrons tend to be confined in the  $\text{In}_{0.53}\text{Ga}_{0.47}\text{As}$ , while holes are confined in the  $\text{GaAs}_{0.51}\text{Sb}_{0.49}$ . Since the periods are only  $\sim 10$ -nm thick, minibands form and an effective band gap that is smaller than either of the two constituent materials is obtained. Fig. 12 shows that with the appropriate surface coating, 150 pairs of  $5$  nm/ $5$  nm of  $\text{In}_{0.53}\text{Ga}_{0.47}\text{As}/\text{GaAs}_{0.51}\text{Sb}_{0.49}$  can have 43% absorption at  $2.23$   $\mu\text{m}$  [51]. Such an absorption region together with a  $0.8$ - $\mu\text{m}$  thick InP multiplication region has been demonstrated in an SAM-APD configuration, as shown in Fig. 13, with an avalanche gain in excess of 30 [52]. The room temperature dark currents reported for a  $44$ - $\mu\text{m}$  diameter device was  $<1$   $\mu\text{A}$  at this level of gain and decreased significantly with temperature. A photoresponse up to  $2.4$   $\mu\text{m}$  was obtained with an external QE of 38% at  $2.2$   $\mu\text{m}$ . An advantage of this material system is that the absorption band edge can be altered simply by varying the thickness of the superlattice period and not the composition. Unfortunately, no excess noise performance has been reported to date in such a system.

### C. $\text{Hg}_{1-x}\text{Cd}_x\text{Te}$ APDs

The band gap of the II–VI material system  $\text{Hg}_{1-x}\text{Cd}_x\text{Te}$  varies from effectively  $0$  eV for  $x = 0.08$  to  $1.4$  eV for CdTe. Early work by Alabedra *et al.* [53] reported on  $\text{Hg}_{1-x}\text{Cd}_x\text{Te}$  APDs with  $x \sim 0.73$  ( $E_g = 0.92$  eV). Hole initiated multiplica-

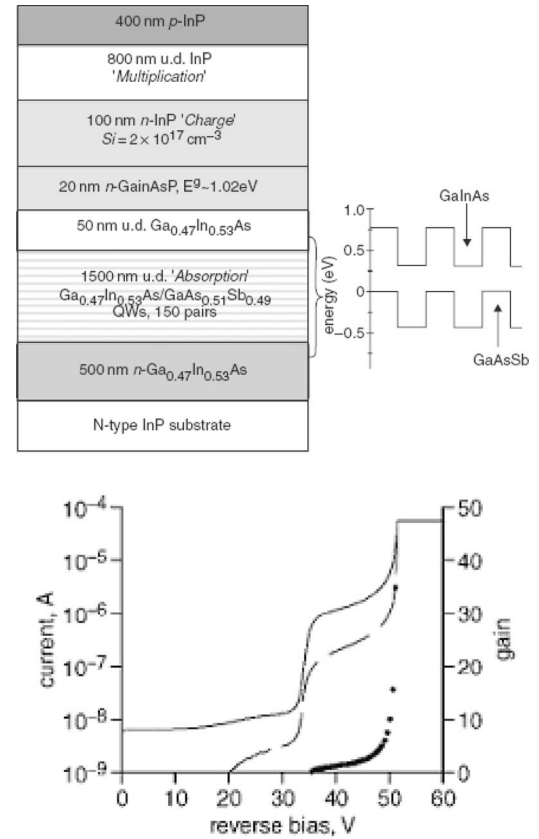


Fig. 13. Schematic device structure of Type II APD on InP substrate and the reverse  $I$ – $V$  and gain at room temperature [52].

tion with  $1.3$   $\mu\text{m}$  illumination gave rise to an excess noise that corresponds to a  $k \sim 10$ . Leveque *et al.* [54] calculated that the  $\beta/\alpha$  ratio changed rapidly with a maximum of 30 for  $x = 0.6$  and a minimum of 0.06 for  $x = 0.41$ . One of the earliest studies of the electron initiated multiplication on a narrow gap  $\text{Hg}_{1-x}\text{Cd}_x\text{Te}$  with a  $11$   $\mu\text{m}$  cutoff and  $300$  K illumination showed that reasonable gains could be obtained at low voltages [55]. Measurements of the noise suggested that only electrons were ionizing.

The lowest reported excess noise to date has been with electron initiated multiplication in  $\text{Hg}_{0.7}\text{Cd}_{0.3}\text{Te}$ , which has a  $77$  K band gap of  $\sim 0.28$  eV or a  $4.4$   $\mu\text{m}$  wavelength cutoff [56], [57]. An almost pure exponential increase in gain with voltage is obtained, as shown in Fig. 14 [57], suggesting that only electrons are undergoing impact ionization. Excess noise measurements on such a structure shows a excess noise that is not only independent of the gain, but has a value of 1, as shown in Fig. 15 [57], suggesting that the electron ionization process is ballistic [58]. Although the results to date have been for only reported in this material system at  $1.55$   $\mu\text{m}$  with a band gap of  $0.28$  eV, and there is no reason why this performance should not extend to much longer wavelengths. Beck *et al.* [59] showed that similar noiseless gain could be obtained with  $\text{Hg}_{1-x}\text{Cd}_x\text{Te}$  corresponding to  $\sim 0.12$  eV ( $10$   $\mu\text{m}$  cutoff) and no tunneling was observed at a bias of  $5$  V, while a gain of 100 was obtained. Wider band gap  $\text{Hg}_{1-x}\text{Cd}_x\text{Te}$  of  $0.56$  eV ( $2.2$   $\mu\text{m}$  cutoff) also showed similar exponential gain behavior however unlike the narrower

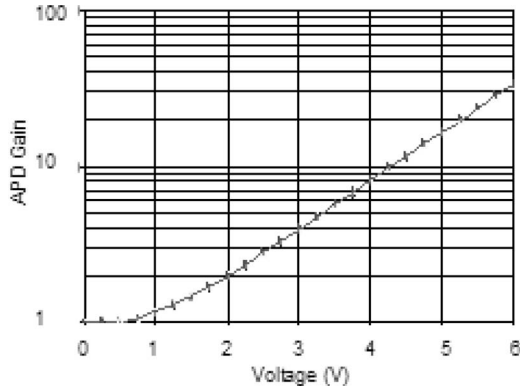


Fig. 14. Measured gain versus voltage for 4.4  $\mu\text{m}$  cutoff HgCdTe APDs at 77 K [57].

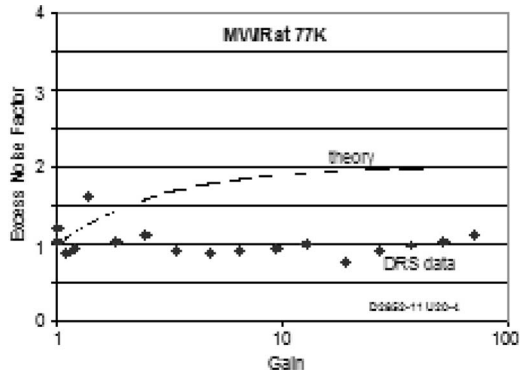


Fig. 15. Excess noise factor versus gain for MWIR ( $E_g = 0.29$  eV at 77 K) APD at 77 K [57].

band gap compositions could be operated at room temperature. The operating voltages were, however, higher and the excess noise was  $F \sim 2$  suggesting that while  $k \sim 0$ , electron-phonon scattering is present. The reason for the extremely low noise in  $\text{Hg}_{1-x}\text{Cd}_x\text{Te}$  for these compositions is attributed to the unique band structure in this material. The higher  $L$  and  $X$  satellite valleys are significantly above the  $\Gamma$  minimum, respectively, and the heavy hole/conduction band mass ratio is  $\sim 30$ . Electrons can therefore gain energy rapidly in the low scattering environment of the  $\Gamma$  valley and impact ionize more readily in the first conduction band without transferring to the higher conduction bands where the scattering rates are significantly higher. This coupled with the large hole scattering rate that prevents holes from impact ionising leads to very large  $\alpha/\beta$  ratio, and hence, low excess noise.

#### D. GaInNAs

The recent development of  $\text{Ga}_{1-x}\text{In}_x\text{N}_y\text{As}_{1-y}$  has attracted considerable interest in emitters and detectors for telecommunication applications on GaAs substrates. The addition of indium to GaAs not only reduces the bandgap, but also increases the lattice parameter, giving rise to strain and limits the total thickness of material that can be grown. Kondow *et al.* [60] showed that adding small amounts of nitrogen continued to decrease the band gap while decreasing the lattice parameter, consequently narrow

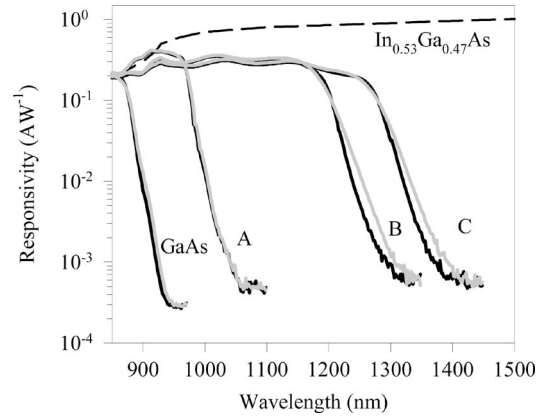


Fig. 16. Room temperature responsivity curves of wafers A, B, and C from Ng *et al.* [63] at 0 and  $-2$  V. Specified and measured responsivity data for a commercial  $\text{In}_{0.53}\text{Ga}_{0.47}\text{As}$  photodiode and an in-house GaAs  $0.5 \mu\text{m}$  p-i-n diode, respectively, are also shown for comparison.

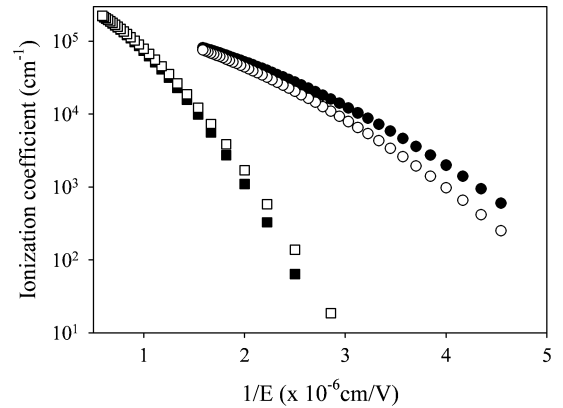


Fig. 17. Experimental GaAs (circles) [67] and InGaP (squares) [68] electron and hole impact ionization coefficients.

bandgap  $\text{Ga}_{1-x}\text{In}_x\text{N}_y\text{As}_{1-y}$  can be grown lattice matched on GaAs substrates provided the In:N ratio is  $\sim 3:1$  [61], [62]. Relatively thick bulk  $\text{Ga}_{1-x}\text{In}_x\text{N}_y\text{As}_{1-y}$  on GaAs has been demonstrated with detection out to  $\sim 1.3 \mu\text{m}$  and responsivities of 110 mA/W [63] for a 400-nm thick absorbing layer (see Fig. 16). It has also been suggested that due to the large effective mass in  $\text{Ga}_{1-x}\text{In}_x\text{N}_y\text{As}_{1-y}$ , the electron ionization coefficients should be suppressed while not affecting those of the holes, giving rise to changes in the  $\beta/\alpha$  ratio [64]. One problem hindering this and the development of  $\text{Ga}_{1-x}\text{In}_x\text{N}_y\text{As}_{1-y}$  detectors generally is that the dark currents appear to be very high and are thought to be related to the formation of nitrogen related defects or traps [65]. There are studies that suggest that annealing or the addition of Sb, which acts as a surfactant and aids the nitrogen incorporation, may reduce the dark currents [65], [66]. Provided  $\text{Ga}_{1-x}\text{In}_x\text{N}_y\text{As}_{1-y}$  can be grown with an effective bandgap of InGaAs and a similar dark current, it may form the basis of an absorber in a SAM-APD structure.

Bulk GaAs is in itself not a particularly suitable avalanche material as the  $\alpha/\beta$  ratio varies from  $\sim 2.5$  to 1.2 over most of the electric fields of interest [67], as can be seen in Fig. 17. Other materials that are lattice matched to GaAs are  $\text{In}_{0.48}\text{Ga}_{0.52}\text{P}$  and

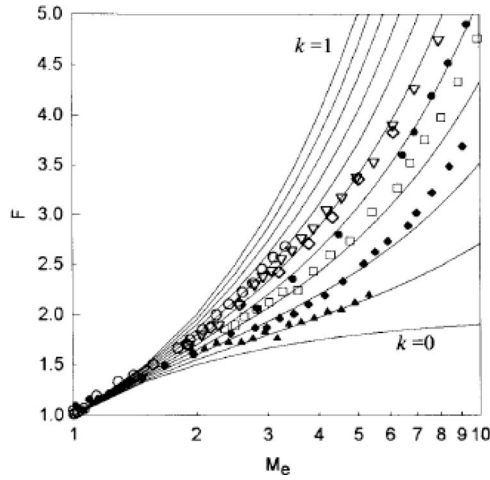


Fig. 18. Excess noise factor versus  $Me$ , for a range of GaAs  $p^+-i-n^+$  structures [69] with nominal avalanche widths  $W = 1.13 \mu\text{m}$  ( $\circ$ ),  $W = 0.57 \mu\text{m}$  ( $\nabla$ ),  $W = 0.49 \mu\text{m}$  ( $\diamond$ ),  $W = 0.28 \mu\text{m}$  ( $\bullet$ ),  $W = 0.20 \mu\text{m}$  ( $\square$ ),  $W = 0.10 \mu\text{m}$  ( $\blacklozenge$ ),  $W = 0.05 \mu\text{m}$  ( $\blacktriangle$ ). Solid lines are McIntyre lines with  $k$  increasing from 0 to 1 in steps of 0.1.

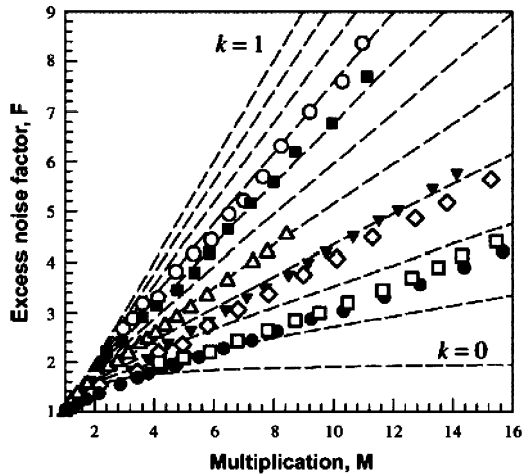


Fig. 19. Excess noise factor for  $\text{Al}_x\text{Ga}_{1-x}\text{As } p^+-i-n^+$  APDs for  $x = 0.4$  ( $\circ$ ),  $0.5$  ( $\blacksquare$ ),  $0.6$  ( $\triangle$ ),  $0.65$  ( $\blacktriangledown$ ),  $0.7$  ( $\diamond$ ),  $0.8$  ( $\square$ ), and  $0.9$  ( $\bullet$ ) [72].

$\text{Al}_x\text{Ga}_{1-x}\text{As}$ .  $\text{In}_{0.48}\text{Ga}_{0.52}\text{P}$  has significantly lower ionization coefficients than GaAs with  $\alpha/\beta \sim 1$  over the entire electric field range investigated (shown in Fig. 17) [68]. Reducing the avalanching width does help to reduce the excess noise in both GaAs [69], [70] and  $\text{In}_{0.48}\text{Ga}_{0.52}\text{P}$  [71] by taking advantage of the dead space effect, as can be seen in Fig. 18 for the case of GaAs [69]. While  $\text{Al}_x\text{Ga}_{1-x}\text{As}$  compositions with  $x < 0.6$  appear not to give any particular advantage as far as the bulk  $\alpha/\beta$  ratios are concerned, at compositions of  $x > 0.7$ , a significant improvement is obtained, as shown in Fig. 19 [72]. The exact mechanism for this sudden increase in  $\alpha/\beta$  ratio is unclear, but it appears to be related to a decrease in the  $\beta$  value rather than an increase in  $\alpha$  Fig. 20 [72]. It is interesting to speculate that at these large Al compositions, it becomes a highly indirect band gap semiconductor like silicon, where the  $\Gamma$  valley is probably unimportant in the ionization process, and the same mechanism responsible for the large  $\alpha/\beta$  ratio in silicon is also responsi-

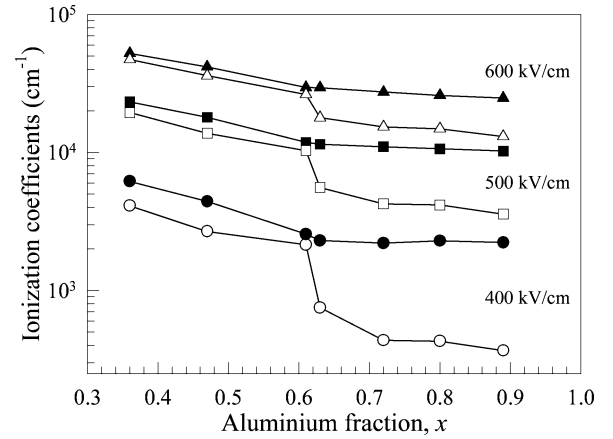


Fig. 20.  $\alpha$  and  $\beta$  taken from Ng *et al.* [72] at different electric fields as a function of the aluminium composition.

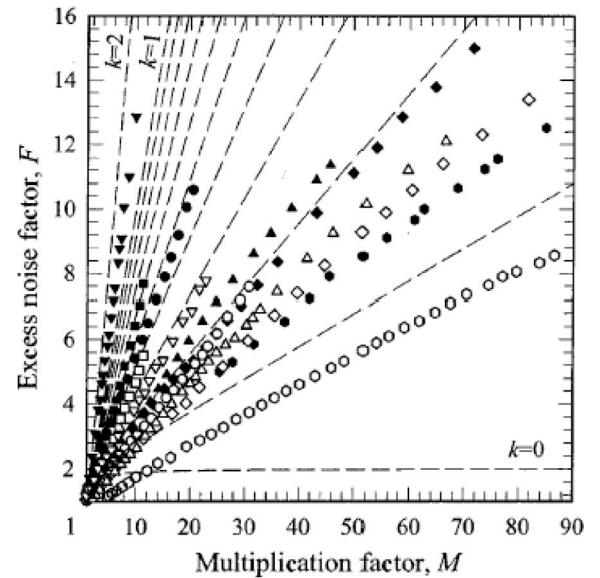


Fig. 21. Excess noise factor ( $F$ ) versus multiplication factor ( $M$ ) measured in  $\text{Al}_{0.8}\text{Ga}_{0.2}\text{As } p-i-n$  diodes [73] with measured  $W$  of  $1.02 \mu\text{m}$  (circles),  $0.82 \mu\text{m}$  (inverted triangles),  $0.31 \mu\text{m}$  (squares),  $0.10 \mu\text{m}$  (triangles),  $0.03 \mu\text{m}$  (diamonds), and  $0.02 \mu\text{m}$  (hexagons). Open and closed symbols are results obtained from pure electron and mixed carrier injection with 442- and 542-nm wavelength light, respectively. Dashed lines are predictions from McIntyre's local model for  $k = 0$  to 1 in steps of 0.1 and  $k = 2$ .

ble for this. It is difficult to see how the sudden change in  $\beta$  between  $x = 0.6 - 0.7$  can follow from the gradual evolution of the band structure with alloy composition, unless an ionization channel suddenly closes, perhaps because the constraints of energy and momentum conservation cannot be satisfied. Due to the wider bandgap in AlGaAs, very thin multiplication regions can be used without tunneling being a problem, and very low noise can be achieved, as shown in Fig. 21 [73], [74]. A  $\text{GaInNAs}/\text{Al}_x\text{Ga}_{1-x}\text{As}$  ( $x > 0.7$ ) structure could form the basis of cheap GaAs-based telecommunication APDs provided the issues of the large dark current in the GaInNAs absorber and the large band gap discontinuity between the materials can be overcome.



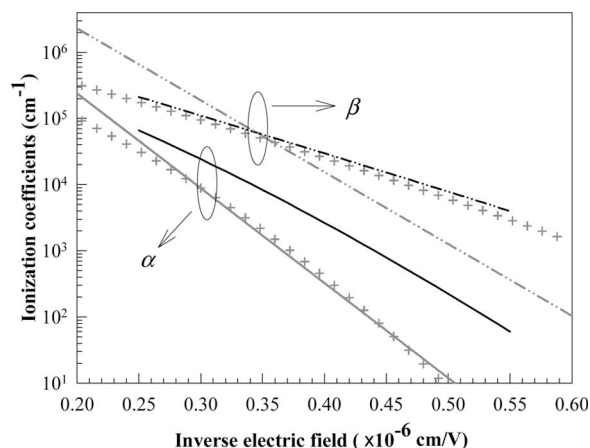


Fig. 22. Ionization coefficients of 4 H-SiC obtained reported by Konstantinov *et al.* (+) [75], Hatakeyama *et al.* (gray lines) [76], and Ng *et al.* (black lines) [77].

## V. ULTRAVIOLET APDs

Silicon carbide (SiC) and gallium nitride (GaN) are promising materials for UV detection due to their wide band gaps. Photodiodes utilizing these materials have the potential to operate at high temperatures with very low leakage currents and should possess good visible-blind or solar-blind performance.

### A. Silicon Carbide

The SiC is technologically more mature and benefits greatly from having a lattice matched SiC substrate. Most of the work on SiC APDs has concentrated on the 4 H polytype, as it has been reported to have widely differing ionization coefficients [75]–[77], as shown in Fig. 22. The large band gap ( $E_g = 3.26$  eV) results in almost an order of magnitude increase in breakdown voltage compared to silicon and much higher electric fields have to be applied before any measurable impact ionization occurs. The first reports of both avalanche gain and excess noise in 4 H SiC were by Ng *et al.* [77] who investigated structures with avalanche widths of 0.1 and 0.28  $\mu\text{m}$ . Due to the fact that 4 H SiC is an indirect band gap semiconductor, the absorption does not increase rapidly above the band edge, and very short wavelengths are required to ensure pure carrier injection into a high field multiplication region [78]. Using different wavelengths of 230–365 nm from a mercury–xenon lamp and a monochromator, multiplication and excess noise measurements were undertaken with results, as shown in Fig. 23(a) and (b) [77]. A  $k$  of  $\sim 0.1$  was obtained in the thinnest device and a slightly larger  $k$  has been reported recently in a thicker structure [79] possibly due to the multiplication being initiated by both electrons and holes. The large asymmetry in ionization coefficients is thought to be due to discontinuities in the electron energy spectrum, whereby electrons cannot reach the threshold energy without phonon collisions or tunneling, and high energy losses of hot carriers due to Bragg reflections from the zone edges [80]. The valence band, by contrast, has a continuous energy spectrum, so that holes can impact ionize much more easily. These results suggest that pure hole-initiated multiplication should give very low excess noise

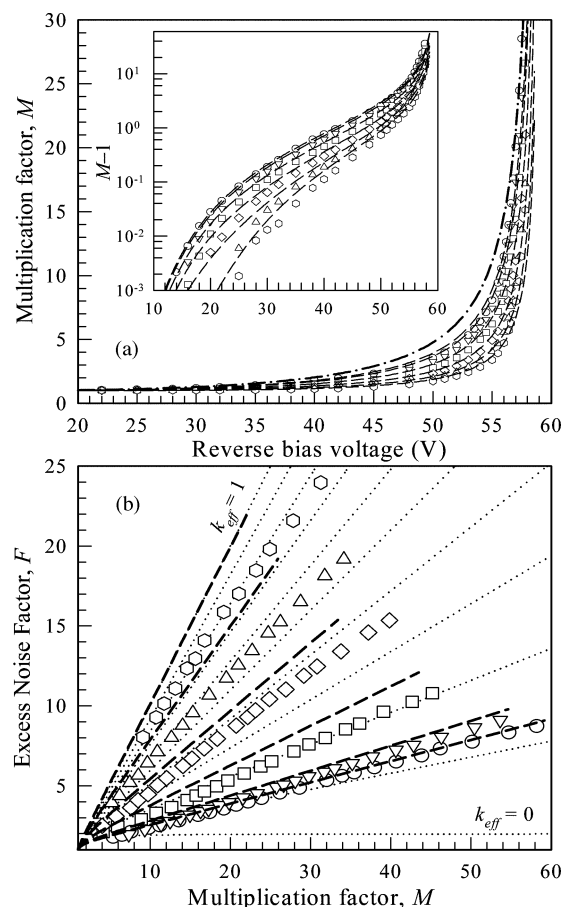


Fig. 23. Measured (symbols) and modeled (dashed lines). (a) Multiplication. (b) Excess noise characteristics of a SiC APD [77] using light of wavelength 230 nm (hexagon), 240 nm ( $\Delta$ ), 250 nm ( $\diamond$ ), 265 nm ( $\square$ ), 297 nm ( $\nabla$ ), and 365 nm ( $\circ$ ). Inset in (a) shows  $(M - 1)$  plotted on a logarithmic scale to accentuate the low multiplication values. Dotted lines in (b) are McIntyre's local prediction for  $k = 0$  to 1 in steps of 0.1.

in thicker avalanching structures; however, very high voltages will be required.

### B. Gallium Nitride

The development of device quality GaN-based APDs has been hampered by the lack of a lattice matched substrate and most epitaxy is undertaken on sapphire or SiC substrates. The high level of dislocations that arise lead to high dark currents at the electric fields at which APDs in this material are expected to operate. One of the earliest reports of reproducible gain in this material was by Yang *et al.* [81] who demonstrated a gain of 23 in a 0.2- $\mu\text{m}$  thick GaN avalanching region with a breakdown voltage of  $\sim 105$  V. The development of hydride vapour phase epitaxy (HVPE) “bulk” GaN substrates has enabled the production of much lower dislocation density GaN structures, and Limb *et al.* [82] have reported 50  $\mu\text{m}$  diameter GaN diodes having an avalanche gain of 1000. The only attempt to measure electron- and hole-initiated multiplication, as well as the associated excess noise, has been undertaken by McClintock *et al.* [83] recently, whereby GaN p–i–n diodes of different thicknesses were grown on AlN templates. They determined that

$\beta$  was larger than  $\alpha$  from both multiplication and excess noise measurements, and that the values were in broad agreement with the theoretical prediction of Oguzman *et al.* [84]. Despite the effort that has gone into making GaN-based APDs, it appears that their performance is far below that of SiC based devices and a true GaN substrate may be required before the promise of GaN UV APDs can be realized.

## VI. CONCLUSION

The developments and improvements in new semiconductor materials has enabled APDs to have the capability to operate across a wide range of wavelengths and for different applications. Earlier APD designs relied on exploitation of large ionization coefficients ratio to achieve low excess noise, leading to the use of thick avalanche regions. While this approach works extremely well in low speed visible wavelength applications using Si APDs, a different excess noise-reduction technique is required for high speed optical communication systems. Low excess noise, due to dead space effect, and high bandwidth, due to reduced carrier transit time, can be achieved using submicron InAlAs or InP avalanche regions with InGaAs absorption regions. However, InGaAs/InAlAs APDs with larger  $\alpha/\beta$  offer lower excess noise, better temperature stability, and higher bandwidth than InGaAs/InP APDs. Materials with large intervalley separation energies and large hole effective mass such as mercury-rich  $\text{Hg}_{1-x}\text{Cd}_x\text{Te}$  have been shown to have large  $\alpha/\beta$  ratio offering low excess noise APDs for infrared applications. For ultraviolet applications SiC offers the most promising characteristics for low excess noise APDs.

## REFERENCES

- [1] S. R. Forrest, "Sensitivity of avalanche photodetector receivers for high bit-rate long-wavelength optical communication systems," in *Semiconductors and Semimetals*, vol. 22. Orlando, FL: Academic, ch. 4, 1985.
- [2] F. Capasso, "Physics of avalanche photodiodes," in *Semiconductors and Semimetals*, vol. 22. Orlando, FL: Academic, ch. 1, 1985.
- [3] R. J. McIntyre, "Multiplication noise in uniform avalanche diodes," *IEEE Trans. Electron. Devices*, vol. ED-13, no. 1, pp. 164–168, Jan. 1966.
- [4] R. B. Emmons, "Avalanche-photodiode frequency response," *J. Appl. Phys.*, vol. 38, no. 9, pp. 3705–3714, Aug. 1967.
- [5] M. M. Hayat, B. E. A. Saleh, and M. C. Teich, "Effect of dead space on gain and noise of double-carrier multiplication avalanche photodiodes," *IEEE Trans. Electron. Devices*, vol. 39, no. 3, pp. 546–552, Mar. 1992.
- [6] R. J. McIntyre, "A new look at impact ionization—Part 1: A theory of gain, noise, breakdown probability and frequency response," *IEEE Trans. Electron. Devices*, vol. 48, no. 8, pp. 1623–1631, Aug. 1999.
- [7] B. Jacob, P. N. Robson, J. P. R. David, and G. J. Rees, "Fokker-Planck model for nonlocal impact ionization in semiconductors," *J. Appl. Phys.*, vol. 90, no. 3, pp. 1314–1317, Aug. 2001.
- [8] D. S. Ong, K. F. Li, G. J. Rees, G. M. Dunn, J. P. R. David, and P. N. Robson, "A Monte Carlo investigation of multiplication noise in thin p+in+ avalanche photodiodes," *IEEE Trans. Electron. Devices*, vol. 45, no. 8, pp. 1804–1810, Aug. 1998.
- [9] S. A. Plimmer, J. P. R. David, D. S. Ong, and K. F. Li, "A simple model including the effects of dead space," *IEEE Trans. Electron. Devices*, vol. 46, no. 4, pp. 769–775, Apr. 1999.
- [10] F. Capasso, W. T. Tsang, A. L. Hutchinson, and G. F. Williams, "Enhancement of electron-impact ionization in a super-lattice—A new avalanche photodiode with a large ionization ratio," *Appl. Phys. Lett.*, vol. 40, no. 1, pp. 38–40, 1982.
- [11] C. K. Chia, B. K. Ng, J. P. R. David, G. J. Rees, R. C. Tozer, M. Hopkinson, R. J. Airey, and P. N. Robson, "Multiplication and excess noise in  $\text{Al}_x\text{Ga}_{1-x}\text{As}/\text{GaAs}$  multilayer avalanche photodiodes," *J. Appl. Phys.*, vol. 94, no. 4, pp. 2631–2637, Aug. 2003.
- [12] S. Wang, F. Ma, X. Li, R. Sidhu, X. G. Zheng, X. Sun, A. L. Holmes, Jr., and J. C. Campbell, "Ultra-low noise avalanche photodiodes with a "centered-well" multiplication region," *IEEE J. Quantum Electron.*, vol. 39, no. 2, pp. 375–378, Feb. 2003.
- [13] S. Wang, J. B. Hurst, F. Ma, R. Sidhu, X. Sun, X. G. Zheng, A. L. Holmes, Jr., J. C. Campbell, A. Huntington, and L. A. Coldren, "Low-noise impact-ionization-engineered avalanche photodiodes grown on InP substrates," *IEEE Photon. Technol. Lett.*, vol. 14, no. 12, pp. 1722–1724, Dec. 2002.
- [14] H. W. Rugg, "An optimized avalanche photodiode," *IEEE Trans. Electron. Devices*, vol. ED-14, no. 5, pp. 239–251, May 1967.
- [15] H. Melchior and W. T. Lynch, "Signal and noise response of high speed germanium avalanche photodiodes," *IEEE Trans. Electron. Devices*, vol. ED-13, no. 12, pp. 820–838, Dec. 1966.
- [16] H. Ando, H. Kanbe, T. Kimura, T. Yamaoka, and T. Kaneda, "Characteristics of germanium avalanche photodiodes in the wavelength region of 1–1.6  $\mu\text{m}$ ," *IEEE J. Quantum. Electron.*, vol. QE-14, no. 11, pp. 804–809, Nov. 1978.
- [17] T. Mikawa, S. Kagawa, T. Kaneda, Y. Toyama, and O. Mikami, "Crystal orientation dependence of ionization rates in germanium," *Appl. Phys. Lett.*, vol. 37, no. 4, pp. 387–389, Aug. 1980.
- [18] W. C. Dash and R. Newman, "Intrinsic optical absorption in single-crystal germanium and silicon at 77 K and 300 K," *Phys. Rev.*, vol. 99, no. 4, pp. 1151–1155, Aug. 1955.
- [19] F. R. Bacher, J. S. Blakemore, J. T. Ebner, and J. R. Arthur, "Optical absorption coefficient of  $\text{In}_{1-x}\text{Ga}_x\text{As}/\text{InP}$ ," *Phys. Rev. B, Condens. Matter*, vol. 37, no. 5, pp. 2551–2557, Feb. 1988.
- [20] D. A. Humphreys and R. J. King, "Measurement of absorption coefficients of  $\text{Ga}_{0.47}\text{In}_{0.53}\text{As}$  over the wavelength range 1.0–1.7  $\mu\text{m}$ ," *Electron. Lett.*, vol. 21, no. 25/26, pp. 1187–1189, Dec. 1985.
- [21] S. R. Forrest, M. Didomenico, R. G. Smith, and H. J. Stocker, "Evidence for tunneling in reverse-biased III–V photodetector diodes," *Appl. Phys. Lett.*, vol. 36, no. 7, pp. 580–582, Apr. 1980.
- [22] J. L. Moll, *Physics of Semiconductors*. New York: McGraw-Hill, 1964.
- [23] S. R. Forrest, R. F. Leheny, R. E. Nahory, and M. A. Pollack, " $\text{In}_{0.53}\text{Ga}_{0.47}\text{As}$  photo-diodes with dark current limited by generation-recombination and tunneling," *Appl. Phys. Lett.*, vol. 37, no. 3, pp. 322–325, May 1980.
- [24] A. Zemel and M. Gallant, "Current–voltage characteristics of metalorganic chemical vapor deposition InP/InGaAs p-i-n photodiodes: The influence of finite dimensions and heterointerfaces," *J. Appl. Phys.*, vol. 64, no. 11, pp. 6552–6561, Dec. 1988.
- [25] J. S. Ng, J. P. R. David, G. J. Rees, and J. Allam, "Avalanche breakdown voltage of  $\text{In}_{0.53}\text{Ga}_{0.47}\text{As}$ ," *J. Appl. Phys.*, vol. 91, no. 8, pp. 5200–5202, Apr. 2002.
- [26] L. J. J. Tan, J. S. Ng, C. H. Tan, and J. P. R. David, "Avalanche noise characteristics in sub-micron InP diodes," *IEEE J. Quantum Electron.*, vol. 44, no. 4, pp. 378–382, Apr. 2008.
- [27] Y. L. Goh, D. J. Massey, A. J. R. Marshall, J. S. Ng, C. H. Tan, W. K. Ng, G. J. Rees, M. Hopkinson, J. P. R. David, and S. K. Jones, "Avalanche multiplication in InAlAs," *IEEE Trans. Electron. Device*, vol. 54, no. 1, pp. 11–16, Jan. 2007.
- [28] K. Nishida, K. Taguchi, and Y. Matsumoto, "InGaAsP heterojunction avalanche photodiodes with high avalanche gain," *Appl. Phys. Lett.*, vol. 35, no. 3, pp. 251–253, Aug. 1979.
- [29] L. W. Cook, G. E. Bulman, and G. E. Stillman, "Electron and hole ionization coefficients in InP determined by photomultiplication measurements," *Appl. Phys. Lett.*, vol. 40, no. 7, pp. 589–591, Apr. 1982.
- [30] H. Kuwatsuka, Y. Kito, T. Uchida, and T. Mikawa, "High-speed InP/InGaAs avalanche photodiodes with a compositionally graded quaternary layer," *IEEE Photon. Technol. Lett.*, vol. 3, no. 12, pp. 1113–1114, Dec. 1991.
- [31] J. C. Campbell, A. G. Dentai, W. S. Holden, and B. L. Kasper, "High performance avalanche photodiode with separate absorption, grading, and multiplication regions," *Electron. Lett.*, vol. 18, no. 20, pp. 818–820, Sep. 1983.
- [32] F. Capasso, A. Y. Cho, and P. W. Foy, "Low-dark-current low-voltage 1.3–1.6  $\mu\text{m}$  avalanche photodiode with high-low electric field profile and separate absorption and multiplication regions by molecular beam epitaxy," *Electron. Lett.*, vol. 20, no. 15, pp. 635–637, Jul. 1984.
- [33] P. Webb, R. McIntyre, J. Scheibling, and M. Holunga, "A planar InGaAs APD fabricated using Si implantation and regrowth techniques," in *Proc. Tech. Dig. Opt. Fiber Conf.*. New Orleans, LA, 1988, p. 129.
- [34] L. E. Tarof, "Planar InP-InGaAs avalanche photodetectors with n-multiplication layer exhibiting a very high gain-bandwidth product," *IEEE Photon. Technol. Lett.*, vol. 2, no. 9, pp. 643–646, Sep. 1990.

- [35] J. C. Campbell, "Recent advances in telecommunications avalanche photodiodes," *J. Lightw. Tech.*, vol. 25, no. 1, pp. 109–121, Jan. 2007.
- [36] P. Yuan, C. C. Hansing, K. A. Anselm, C. V. Lenox, H. Nie, A. L. Holmes, Jr., B. G. Streetman, and J. C. Campbell, "Impact ionization characteristics of III–V semiconductors for a wide range of multiplication region thicknesses," *IEEE J. Quantum Electron.*, vol. 36, no. 2, pp. 198–204, Feb. 2000.
- [37] J. S. Ng, C. H. Tan, J. P. R. David, G. Hill, and G. J. Rees, "Field dependence of impact ionization coefficients in  $\text{In}_{0.53}\text{Ga}_{0.47}\text{As}$ ," *IEEE Trans. Electron. Device.*, vol. 50, no. 4, pp. 901–905, Apr. 2003.
- [38] D. Ritter, R. A. Hamm, A. Feyngenson, and M. B. Panish, "Anomalous electric-field and temperature-dependence of collector multiplication in  $\text{InP}/\text{Ga}_{0.47}\text{In}_{0.53}\text{As}$  heterojunction nipolar-transistors," *Appl. Phys. Lett.*, vol. 60, no. 25, pp. 3150–3152, Jun. 1992.
- [39] J. S. Ng, C. H. Tan, J. P. R. David, and G. J. Rees, "Effect of impact ionization in the  $\text{InGaAs}$  absorber on excess noise of avalanche photodiodes," *IEEE J. Quantum Electron.*, vol. 41, no. 8, pp. 1092–1096, Aug. 2005.
- [40] F. Capasso, K. Mohammed, K. Alavi, A. Y. Cho, and P. W. Foy, "Impact ionization rates for electrons and holes in  $\text{Al}_{0.48}\text{In}_{0.52}\text{As}$ ," *Appl. Phys. Lett.*, vol. 45, no. 9, pp. 968–970, 1984.
- [41] I. Watanabe, T. Torikai, K. Makita, K. Fukushima, and T. Uji, "Impact ionization rates in  $(1\ 0\ 0)\ \text{Al}_{0.48}\text{In}_{0.52}\text{As}$ ," *IEEE Electron Device Lett.*, vol. 11, no. 10, pp. 437–438, Oct. 1990.
- [42] C. Lennox, P. Yuan, H. Nie, O. Baklenov, J. C. Campbell, A. L. Homes, Jr., and B. G. Streetman, "Thin multiplication region  $\text{InAlAs}$  homojunction avalanche photodiodes," *Appl. Phys. Lett.*, vol. 73, no. 6, pp. 783–784, 1998.
- [43] Y. L. Goh, A. R. J. Marshall, D. J. Massey, J. S. Ng, C. H. Tan, M. Hopkinson, J. P. R. David, S. K. Jones, C. C. Button, and S. M. Pinches, "Excess avalanche noise in  $\text{In}_{0.52}\text{Al}_{0.48}\text{As}$ ," *IEEE J. Quantum Electron.*, vol. 43, no. 5–6, pp. 503–507, May 2007.
- [44] E. Yagyu, E. Ishimura, M. Nakaji, T. Aoyagi, and Y. Tokuda, "Simple planar structure for high-performance  $\text{AlInAs}$  avalanche photodiodes," *IEEE Photon. Technol. Lett.*, vol. 18, no. 1, pp. 76–78, Jan. 2006.
- [45] X. G. Zheng, P. Yuan, X. Sun, G. S. Kinsey, A. L. Holmes, B. G. Streetman, and J. C. Campbell, "Temperature dependence of the ionization coefficients of  $\text{Al}_x\text{Ga}_{1-x}\text{As}$ ," *IEEE J. Quantum Electron.*, vol. 36, no. 10, pp. 1168–1173, Oct. 2000.
- [46] C. Groves, R. Ghin, J. P. R. David, and G. J. Rees, "Temperature dependence of impact ionization in  $\text{GaAs}$ ," *IEEE Trans. Electron. Device.*, vol. 50, no. 10, pp. 2027–2031, Oct. 2003.
- [47] B. F. Levine, R. N. Sacks, J. Ko, M. Jazwiecki, J. A. Valdmanis, D. Gunther, and J. H. Meier, "A new planar  $\text{InGaAs-InAlAs}$  avalanche photodiode," *IEEE Photon. Technol. Lett.*, vol. 18, no. 18, pp. 1898–1900, Sep. 2006.
- [48] A. R. Hawkins, T. E. Reynolds, D. R. England, D. I. Babic, M. J. Mondry, K. Streubel, and J. E. Bowers, "Silicon heterointerface photodetector," *Appl. Phys. Lett.*, vol. 68, no. 26, pp. 3692–3694, Jun. 1996.
- [49] Y. Kang, P. Mages, A. R. Clawson, P. K. L. Yu, M. Bitter, Z. Pan, A. Pauchard, S. Hummel, and Y. H. Lo, "Fused  $\text{InGaAs-Si}$  avalanche photodiodes with low-noise performances," *IEEE Photon. Technol. Lett.*, vol. 14, no. 11, pp. 1593–1595, Nov. 2002.
- [50] O. V. Sulima, M. G. Mauk, Z. A. Shellenbarger, J. A. Cox, J. V. Li, P. E. Sims, S. Datta, and S. B. Rafol, "Uncooled low voltage  $\text{AlGaAsSb/InGaAsSb/GaSb}$  avalanche photodetectors," *Proc. Int. Elect. Eng. Optoelectron.*, vol. 15, no. 1, pp. 1–5, 2004.
- [51] R. Sidhu, N. Duan, J. C. Campbell, and A. L. Holmes, Jr., "A long-wavelength photodiode on  $\text{InP}$  using lattice-matched  $\text{GaInAs-GaAsSb}$  Type-II quantum wells," *IEEE Photon. Technol. Lett.*, vol. 17, no. 12, pp. 2715–2717, Dec. 2005.
- [52] R. Sidhu, L. Zhang, N. Tan, N. Duan, J. C. Campbell, A. L. Holmes, Jr., C.-F. Hsu, and M. A. Itzler, "2.4  $\mu\text{m}$  cutoff wavelength avalanche photodiode on  $\text{InP}$  substrate," *Electron. Lett.*, vol. 42, no. 3, Feb. 2006.
- [53] R. Alabedra, B. Orsal, G. Lecoy, G. Pichard, J. Meslage, and P. Fragnon, "An  $\text{Hg}_{0.3}\text{Cd}_{0.7}\text{Te}$  avalanche photodiode for optical—Fiber transmission-systems at  $\lambda = 1.3\ \mu\text{m}$ ," *IEEE Trans. Electron. Devices*, vol. 2, no. 7, pp. 1302–1306, Jul. 1985.
- [54] G. Leveque, M. Nasser, D. Bertho, B. Orsal, and R. Alabedra, "Ionization energies in  $\text{Cd}_x\text{Hg}_{1-x}\text{Te}$  avalanche photodiodes," *Semicon. Sci. Technol.*, vol. 8, no. 7, pp. 1317–1323, Jul. 1993.
- [55] C. T. Elliott, N. T. Gordon, R. S. Hall, and G. Crimes, "Reverse breakdown in long wavelength lateral collection  $\text{Cd}_x\text{Hg}_{1-x}\text{Te}$  diodes," *J. Vacuum Sci. Technol.*, vol. 8, no. 2, pp. 1251–1253, Mar–Apr. 1990.
- [56] J. D. Beck, C. F. Wan, M. A. Kinch, and J. E. Robinson, "MWIR  $\text{HgCdTe}$  avalanche photodiodes," *Proc. SPIE*, vol. 4454, pp. 188–197, 2001.
- [57] M. A. Kinch, J. D. Beck, C. F. Wan, F. Ma, and J. Campbell, " $\text{HgCdTe}$  electron avalanche photodiodes," *J. Electron. Mater.*, vol. 33, no. 6, pp. 630–639, Jun. 2004.
- [58] F. Ma, X. Li, J. C. Campbell, J. D. Beck, C.-F. Wan, and M. A. Kinch, "Monte Carlo simulations of  $\text{Hg}_{0.7}\text{Cd}_{0.3}\text{Te}$  avalanche photodiodes and resonance phenomenon in the multiplication noise," *Appl. Phys. Lett.*, vol. 83, no. 4, pp. 785–787, Jul. 2003.
- [59] J. D. Beck, C.-F. Wan, M. A. Kinch, J. E. Robinson, F. Ma, and J. C. Campbell, "The  $\text{HgCdTe}$  electron avalanche photodiode," *J. Electron. Mater.*, vol. 35, no. 6, pp. 1166–1173, Jun. 2006.
- [60] M. Kondow, K. Uomi, A. Niwa, T. Kitatani, S. Watahiki, and Y. Yazawa, " $\text{GaInAs}$ : A novel material for long-wavelength-range laser diodes with excellent high-temperature performance," *Jpn. J. Appl. Phys.*, vol. 35, Part 1, no. 2B, pp. 1273–1275, Feb. 1996.
- [61] S. Sato, Y. Osawa, and T. Saitoh, "Room temperature operation of  $\text{GaInAs/GaInP}$  double-heterostructure laser diodes grown by metalorganic chemical vapor deposition," *Jpn. J. Appl. Phys.*, vol. 36, Part 1, no. 5A, pp. 2671–2675, May 1997.
- [62] L. Bellaiche, "Band gaps of lattice-matched  $(\text{Ga},\text{In}) (\text{As},\text{N})$  alloys," *Appl. Phys. Lett.*, vol. 75, no. 17, pp. 2578–2580, Oct. 1999.
- [63] J. S. Ng, W. M. Soong, M. J. Steer, M. Hopkinson, J. P. R. David, J. Chamings, S. J. Sweeney, and A. R. Adams, "Long wavelength bulk  $\text{GaInAs}$  p-i-n photodiodes lattice matched to  $\text{GaAs}$ ," *J. Appl. Phys.*, vol. 101, Article no. 064506, 2007.
- [64] A. R. Adams, "Band-structure engineering to control impact ionisation and related high-field processes," *Elec. Lett.*, vol. 40, no. 17, pp. 1086–1088, Aug. 2004.
- [65] R. J. Kaplar, D. Kwon, S. A. Ringel, A. A. Allerman, S. R. Kurtz, E. D. Jones, and R. M. Sieg, "Deep levels in p- and n-type  $\text{InGaAsN}$  for high-efficiency multi-junction III–V solar cells," *Solar Energy Mater. Solar Cells*, vol. 69, no. 1, pp. 85–91, Aug. 2001.
- [66] W. K. Cheah, W. J. Fan, S. F. Yoon, D. H. Zhang, B. K. Ng, W. K. Loke, R. Liu, and A. T. S. Wee, " $\text{GaAs}$ -based heterojunction p-i-n photodetectors using pentanary  $\text{InGaAsNSb}$  as the intrinsic layer," *IEEE Photon. Technol. Lett.*, vol. 17, no. 9, pp. 1932–1934, Sep. 2005.
- [67] G. E. Bulman, V. M. Robbins, and G. E. Stillman, "The determination of impact ionization coefficients in  $(1\ 0\ 0)$  gallium-arsenide using avalanche noise and photocurrent multiplication measurements," *IEEE Trans. Electron. Devices*, vol. 32, no. 11, pp. 2454–2466, Nov. 1985.
- [68] R. Ghin, J. P. R. David, S. A. Plimmer, M. Hopkinson, G. J. Rees, D. C. Herbert, and D. R. Wright, "Avalanche multiplication and breakdown in  $\text{Ga}_{0.52}\text{In}_{0.48}\text{P}$  diodes," *IEEE Trans. Electron. Devices*, vol. 45, no. 10, pp. 2096–2101, Oct. 1998.
- [69] K. F. Li, D. S. Ong, J. P. R. David, G. J. Rees, R. C. Tozer, P. N. Robson, and R. Grey, "Avalanche multiplication noise characteristics in thin  $\text{GaAs}$  p+i-n +diodes," *IEEE Trans. Electron. Dev.*, vol. 45, no. 10, pp. 2102–2107, Oct. 1998.
- [70] X. Li, X. Zheng, S. Wang, F. Ma, and J. C. Campbell, "Calculation of gain and noise with dead space for  $\text{GaAs}$  and  $\text{Al}_x\text{Ga}_{1-x}\text{As}$  avalanche photodiodes," *IEEE Trans. Electron Devices*, vol. 49, no. 7, pp. 1112–1117, Jul. 2002.
- [71] C. H. Tan, R. Ghin, J. P. R. David, G. J. Rees, and M. Hopkinson, "The effect of dead space on gain and excess noise in  $\text{In}_{0.48}\text{Ga}_{0.52}\text{P}^+\text{in}^+$  diodes," *Semicon. Sci. Technol.*, vol. 18, pp. 803–806, 2003.
- [72] B. K. Ng, J. P. R. David, G. J. Rees, R. C. Tozer, M. Hopkinson, and R. J. Riley, "Avalanche multiplication and breakdown in  $\text{Al}_x\text{Ga}_{1-x}\text{As}$  ( $x < 0.9$ )," *IEEE Trans. Electron Devices*, vol. 49, no. 12, pp. 2349–2351, Dec. 2002.
- [73] B. K. Ng, J. P. R. David, R. C. Tozer, M. Hopkinson, G. Hill, and G. J. Rees, "Excess noise characteristics of  $\text{Al}_{0.8}\text{Ga}_{0.2}\text{As}$  avalanche photodiodes," *IEEE Photon. Technol. Lett.*, vol. 14, no. 4, pp. 522–524, Apr. 2002.
- [74] X. G. Zheng, X. Sun, S. Wang, P. Yuan, G. S. Kinsey, A. L. Holmes, Jr., B. G. Streetman, and J. C. Campbell, "Multiplication noise of  $\text{AlGaAs}$  avalanche photodiodes with high  $\text{Al}$  concentration and thin multiplication region," *Appl. Phys. Lett.*, vol. 78, pp. 3833–3835, Jun. 2001.
- [75] A. O. Konstantinov, Q. Wahab, N. Nordell, and U. Lindefelt, "Ionization rates and critical fields in 4H silicon carbide," *Appl. Phys. Lett.*, vol. 71, no. 1, pp. 90–92, Jul. 1997.
- [76] T. Hatakeyama, T. Watanabe, T. Shinohe, K. Kojima, K. Arai, and N. Sano, "Impact ionization coefficients of 4H-SiC," *Appl. Phys. Lett.*, vol. 85, no. 8, pp. 1380–1382, Aug. 2004.
- [77] B. K. Ng, J. P. R. David, R. C. Tozer, G. J. Rees, F. Yan, J. H. Zhao, and M. Weiner, "Nonlocal effects in thin 4H-SiC UV avalanche photodiodes," *IEEE Trans. Electron Devices*, vol. 50, no. 8, pp. 1724–1732, Aug. 2003.

- [78] S. G. Sridhara, T. J. Eperjesi, R. P. Devaty, and W. J. Choyke, "Penetration depths in the ultraviolet for 4 H, 6 H and 3 C silicon carbide at seven common laser pumping wavelengths," *Mater. Sci. Eng. B-Solid State Mater. Adv. Technol.*, vol. 61–62, pp. 229–233, Jul. 1999.
- [79] X. Y. Guo, A. L. Beck, Z. H. Huang, N. Duan, J. C. Campbell, D. Emerson, and J. J. Sumakeris, "Performance of low-dark-current 4H-SiC avalanche photodiodes with thin multiplication layer," *IEEE Trans. Electron Devices*, vol. 53, no. 9, pp. 2259–2265, Sep. 2006.
- [80] A. O. Konstantinov, Q. Wahab, N. Nordell, and U. Lindefelt, "Study of avalanche breakdown and impact ionization in 4H silicon carbide," *J. Electronic Mater.*, vol. 27, no. 4, pp. 335–341, Apr. 1998.
- [81] B. Yang, T. Li, K. Heng, C. Collins, S. Wang, J. C. Carrano, R. D. Dupuis, J. C. Campbell, M. J. Schurman, and I. T. Ferguson, "Low dark current GaN avalanche photodiodes," *IEEE J. Quantum Electron.*, vol. 36, no. 12, pp. 1389–1391, Dec. 2000.
- [82] J. B. Limb, D. Yoo, J. H. Ryou, W. Lee, S. C. Shen, R. D. Dupuis, M. L. Reed, C. J. Collins, M. Wraback, D. Hanser, E. Preble, N. M. Williams, and K. Evans, "GaN ultraviolet avalanche photodiodes with optical gain greater than 1000 grown on GaN substrates by metal-organic chemical vapor deposition," *Appl. Phys. Lett.*, vol. 89, no. 1, Article no. 011112, Jul. 2006.
- [83] R. McClintock, J. L. Pau, K. Miner, C. Bayram, P. Kung, and M. Razeghi, "Hole-initiated multiplication in back-illuminated GaN avalanche photodiodes," *Appl. Phys. Lett.*, vol. 90, no. 14, Article no. 141112, Apr. 2007.
- [84] I. H. Oguzman, E. Bellotti, K. F. Brennan, J. Kolnik, R. Wang, and P. P. Ruden, "Theory of hole initiated impact ionization in bulk zincblende and wurtzite GaN," *J. Appl. Phys.*, vol. 81, no. 12, pp. 7827–7834, Dec. 1997.

**J. P. R. David** (SM'96) received the B.Eng. and Ph.D. degrees in electronic engineering from the University of Sheffield, Sheffield, U.K.

During 1985, he was with the Central Facility for III–V Semiconductors, Sheffield, where he was involved in the characterization activity. During 2001, he was with Marconi Optical Components (now Bookham Technologies). He is currently a Professor at the Department of Electronic and Electrical Engineering, University of Sheffield. His current research interests include piezoelectric III–V semiconductors and impact ionization in analogue and single-photon avalanche photodiodes.

Dr. David was an IEEE Lasers and Electro Optics Society (LEOS) Distinguished Lecturer from 2002 to 2004.

**C. H. Tan** (M'95) received the B.Eng. and Ph.D. degrees in electronic engineering from the Department of Electronic and Electrical Engineering, University of Sheffield, Sheffield, U.K., in 1998 and 2002, respectively.

Since 2003, he has been with the Department of Electronic and Electrical Engineering, University of Sheffield, where he was earlier a Lecturer, and currently, a Senior Lecturer. He has extensive experience in characterization and modeling of high speed low noise avalanche photodiodes and phototransistors. His current research interests include single photon avalanche diodes, mid-infrared photodiodes, quantum dot infrared detectors, and ultrahigh speed avalanche photodiodes and phototransistors.